Algerian Journal of Environmental Science and Technology
December edition. Vol.9. N°4. (2023)
ISSN : 2437-1114
www.aljest.org

Formation environment of whiteschists from the Ti-N-Eggoleh region (Serouenout terrane, Central Hoggar): Petrographic, Mineralogical study and Estimation of P-T conditions.

A. Bitam-Derridj[1*], Z. Adjerid[2,3] , K. Ouzegane[3]

[1] Laboratoire ressources minérales et énergetiques, Faculté des hydrocarbures et de la chimie. Université M'hamed Bouguera, Avenue de l'Indépendance, 35000, Boumerdès.
[2] Ecole Normale Supérieure (Département des Sciences Naturelles). B.P. 92-Vieux Kouba. 16308-Alger. Algérie
[3] Lab. de Géodynamique. Géologie de l'Ingénieur et de Planétologie. FSTGAT-U.S.T.H.B. B.P. 32. El Alia. Dar el Beida. 16111-Alger- Algérie

*Corresponding author: a.derridj@univ-boumerdes.dz; Tel.: +213 24 795254; Fax: +213 24 795280

ARTICLE INFO

Article History :
*Received : **21/07/2022***
*Accepted : **03/11/2022***

***Key Words**:*

Whiteschists; Ti-N-Eggoleh; high-pressure environment: talc-kyanite-quartz.

ABSTRACT/RESUME

Abstract: *Coarse-grained whiteschists (talc-kyanite rocks), containing the high-pressure environment talc-kyanite-quartz ± phengite assemblage (~ 20 kbar and 600°C) are abundant in the Ti-N-Eggoleh region.*

Texturally these whiteschists show breakdown of talc + kyanite + quartz to cordierite in silica-rich samples during decreasing pressure (~ 10 kbar and ~ 700°C), whereas kyanite + talc react to allow the growth of cordierite-sapphirine symplectites with increasing temperature (8-10 kbar and ~ 800°C), or cordierite + corundum in silica-poor microdomains during the cooling stage (~ 600°C).

The metamorphic evolution of these M(F)ASH rocks are consistent with the closure of an oceanic basin that likely occurred during the Pan-African orogeny that developed during the assembly of the supercontinent Gondwana between 750 and 500 Ma.

I. Introduction

Talc-rich kyanite-bearing schists or Whiteschists are high-pressure rocks (>10kbar). Major element analyses define these rocks within the relatively simple MgO, Fe_2O_3, Al_2O_3, SiO_2 and H_2O (MFASH) metamorphic rocks that contain talc- and kyanite (± quartz or coesite) as equilibrium phases. Some investigators [1] extended this domain to include coesite-pyrope quartzites, which they regard as ultrahigh-pressure protoliths of high-pressure talc-rich schists.

Whiteschists develop by the extreme metasomatic alteration of common rock-types, by elimination of mobile elements such as alkali elements, CaO, FeO, MnO, P_2O_5, Rb, Ba, etc, during metamorphism.

The talc-rich schists protolith is difficult to identify, due to extensive geochemical and textural metasomatic alteration; however, the usual known have been interpreted to be meta-sediments or volcanic deposits [2, 3]. Recent studies indicate that some examples have mafic -meta-basalt [4, 5, 6], granite [7, 8] or a mixture of acid and mafic/ultramafic precursors [9], having undergone high-pressure, extreme metasomatic process.

According to Franz [10], the production of whiteschists occurs in a wide stability environment, which strongly depends on the chemical composition of the protolith that requires elevated contents of Al and Mg as well as low Fe, Ca, and Na contents and depends on XCO_2 and fO_2.

The major aim of this work is to present textural, mineralogical and the *P-T* environment of talc-rich schists from the Ti-N-Eggoleh region (Central Hoggar). The significance of the results will be discussed in a regional context, trying to throw some light on the evolution of the Hoggar shield.

II. Materials and methods

II.1. Geologic outline

The Tuareg Shield comprises the Hoggar, the Aïr and the Ifors cratons (**Fig. 1**). It represents a part of the Trans-Saharan Pan-African orogenic belt that runs from the Atlantic Ocean (Nigerian Shield) in the south towards the Alpine Atlas Belt to the north with a surface of 550,000 km^2. It is made of Precambrian rocks surrounded by Paleozoic sediments deposited after the end of the Pan-African orogeny.

The Tuareg Shield is composed of 25 displaced terranes that are separated by subvertical strike-slip shear zones or major thrust fronts [11], (**Fig. 1**). These terranes, amalgamated together during the Pan-African orogenic cycle between 870 and 540 Ma, have different origins and are composed of either variably reworked Archaean to Paleoproterozoic domains [12], or of juvenile Neoproterozoic units [13, 14, 15, 16,17]. During the final collisional stage at 630-580 Ma, the Tuareg Shield was compressed between the West African craton (WAC) to the west and the Saharan metacraton to the east during the Pan-African orogeny due to the closure of a large ocean (18, 19, 15, 12, 11].

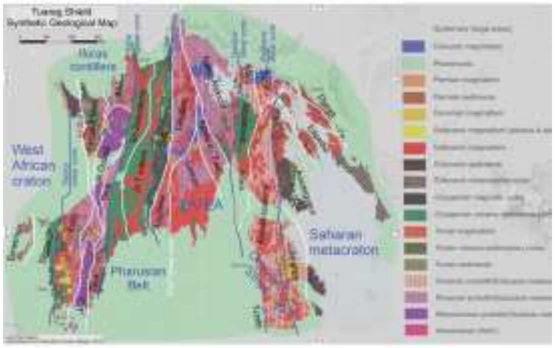

__Fig 1.__ Synthetic geological map of the Tuareg Shield with the delimitation of the 25 terranes [11].

The Tuareg Shield is subdivided into three parts, with the western part being mostly juvenile and Neoproterozoic in age, the eastern part being of more enigmatic origin and possibly related to an eastern craton, and the central part being dominated by old metamorphic lithologies that are intruded by abundant 630–580 Ma granitoid plutons and batholiths [20, 21].

The central Hoggar mainly comprises the LATEA (Laouni, Azrou N'Fad, Tefedest, Egéré and Aleksod) “metacraton” (**Fig. 1**), which includes several Proterozoic and Archaean terranes. The western and eastern margins of the LATEA are now delimited by a series of oceanic origin [15]: the Iskel Terrane, to the west (**Fig. 1**) and the juvenile Neoproterozoic Sérouènout Terrane, to the east (**Fig. 1**) that comprises kyanite + talc-rich schist and eclogitic assemblage lithologies [22, 23, 9].

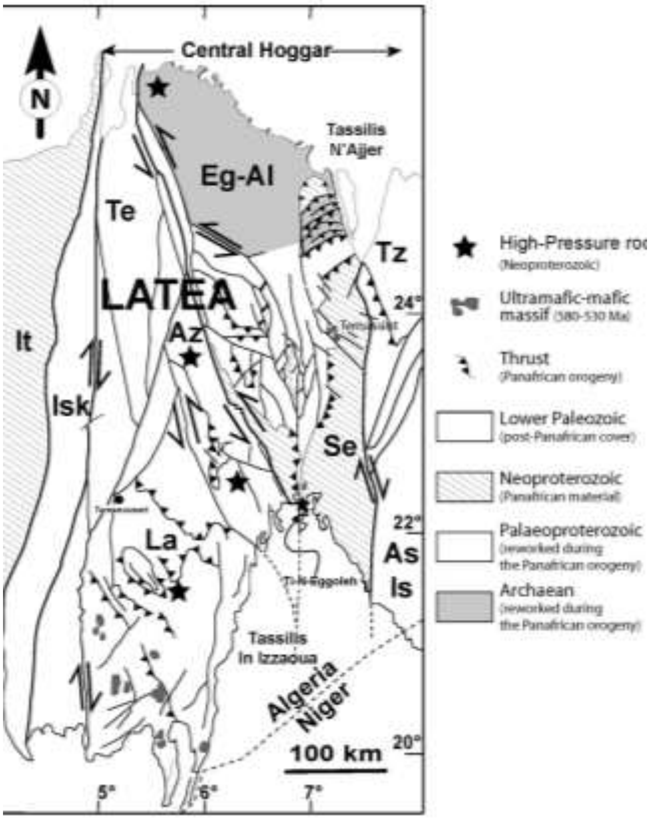

__Fig 2.__ Geological sketch map of the Central Hoggar, adapted from [15].

The only high-P rocks (eclogites) reported so far in the Sérouènout terrane (See in **Fig. 2**) have been observed in the Ti-N-Eggoleh area [23, 9, 22].

This area (**Fig. 3**) is also made up of a complex mixture of carbonaceous metasediments, peridotites, whiteschists (i.e. kyanite + talc schists), chlorite schists and hydrothermal sulphide ores reminiscent of an “ophiolitic mélange” metamorphosed under eclogite-facies conditions.

The Ti-N-Eggoleh region comprises distinct series, which are in agreement with those previously reported by Guérangé [24], but with a much greater degree of metamorphism, resulting from a complex evolution model. The exceptional nature of the outcrops allows highlighting a sequence of metasedimentary or basic gneisses crossed by an important system of late dolerite veins, gabbroic sills and peridotites (**Fig. 3**). Numerous granite types displaying various petrographic features are also present in the ground. The paleo basement, which is most likely the older unit, is rarely exposed. It corresponds to biotite or amphibole-bearing migmatitic gneisses which form isolated limbs and often covered by recent sedimentary deposits (Tassili).

Fig 3. *Outcrop mode of whiteschists and associated rocks in the Ti-N-Eggoleh hills*

The cover series are varied, but three major types can be distinguished. These involve a thick schist series, comprising talc schists and chlorite schists associated with extensive calcomagnesian and greenstone sequences.

The serpentinite greenstones are often traversed by veins of calcite, giving the ophicalcite appearance to most of the outcrops of these greenstone rocks. Consequently, it is usually hard to distinguish marble from serpentinite.

The cover series include also other less frequent rock types as calcareous quartz-calcite-dolomite sandstones and kyanite-rich corindonites. To these formations are associated high-pressure eclogites [22].

Marbles are present as small lenses, on the flat relief of the region, or occupy vast areas that can cover several hundred meters squared around Oued Tigueleï. These are white bluish or pinkish marbles, colored occasionally by spinel and corundum.

Other dense marble bodies are also mapped in this region. They are particular by the unusual presence of hibonite, which occurs exclusively in high temperature environments.

The dominant rock in the Ti-N-Eggoleh area is talc-kyanite rich schist that develops exclusively in Mg-rich systems of high-pressure environments.

III. Results and discussion

III.1. Petrography

Talc schists or whiteschists from the Ti-N-Eggoleh region are widespread (**Figs. 3** and **4**). They include the rare mineral assemblage talc (Tlc) + kyanite (Ky) ± quartz (Qtz) that requires high-P environments for its growth (**Fig 5a**). Amphibole (Amph), phengite (Phn) and chlorite (Chl) are minor phases in these rocks (**Fig. 5b**) and cordierite (Crd), sapphirine (Spr) and corundum (Cor) are mostly related to late-stage corona textures and symplectites (**Figs. 5c** and **d**).

The mineralogy of whiteschists is basic but variable. This may explain their possible transition to chlorite schists or even to chlorite quartzites, when the size of talc reduces or totally disappears [25].

The prevalent presence of remnant quartz grains (**Fig. 5a**) would suggest that it is a principal reactant in achieving equilibrium leading to the occurrence of talc and kyanite. The other reacting mineral must be ferromagnesian to attain the chemical equilibrium.

According to observed textures, the additional reactant was consumed in significant proportions during initial equilibrium, since its traces are no longer found in most samples.

Chlorite, considered as a potential candidate for this equilibrium (**R**$_1$), is observed in some quartz-poor samples. So, the most likely balancing is as follows:

3 Chl + 16 Qtz ➔ 4 Tlc + 6Ky
(**R**$_1$).

This reaction, first reported by Schreyer & Abraham [26] is widely accepted now days to account the stable talc-kyanite (± quartz) assemblage in most whiteschist deposits.

The development of cordierite among early paragenesis minerals (**Fig. 5a**) occurs as a result of changing stability conditions in the rock (**R**$_2$). This reaction is only common in silica-rich microdomains and takes place as follows:

Tlc + Ky + Qtz ⇒ Crd(**R**$_2$).

	1	Ta ($Si_{7.983}Al_{0.116}Ti_{0.000}Fe_{0.074}Mn_{0.005}Mg_{5.763}Ca_{0.004}Na_{0.025}K_{0.000}F_{0.009}Cl_{0.001}H_{3.899}O_{24}$)
Tlc +	5.8687	Ky ($Si_1Al_2O_5$)
Ky +	0.9656	Qtz (SiO_2)
Qtz	0.1110	O
⇒	2.9631	Crd ($Si_{5.000}Al_{4.000}Ti_{0.003}Fe_{0.024}Mn_{0.000}Mg_{1.945}Ca_{0.005}Na_{0.027}K_{0.007}O_{18}$)
Crd +	1.9499	Fluid (H_2O)
H_2O		*R* ($Si_{0.000}Al_{0.000}Ti_{-0.009}Cr_{0.000}Fe_{0.004}Mn_{0.005}Mg_{0.001}Ca_{-0.012}Na_{-0.055}K_{-0.023}F_{0.099}Cl_{0.001}$)

Fig 4. *Outcrop type of Ti-N-Eggoleh whiteschists in the field. (a) They occur as spheres and as metric beds on the elevated hills, and (b) as several hundred metre long lodes on the reg.*

Only rare whiteschist outcrops contain talc-kyanite-quartz. Most of the rocks are talc-kyanite and generally are replaced by cordierite-saphirine and/or corundum symplectites.

Considering the observed textures, too, the growth of sapphire-cordierite-corundum assemblages could occur secondarily (**Figs. 5 c** and **d**), due to another late change in the P-T environment. This led to instability of talc and kyanite and the growth of cordierite-saphirine (**R**$_3$) and/or cordierite-corundum symplectites (**R**$_4$). The following paragenetic sequence can be retained in this case:

Tlc + Ky ⇒ Crd + Spr (**R**$_3$),

	1	Ta ($Si_{7.973}Al_{0.351}Ti_{0.005}Fe_{0.086}Mn_{0.003}Mg_{5.380}Ca_{0.027}Na_{0.028}K_{0.008}F_{0.008}Cl_{0.005}H_{3.987}O_{24}$)
Tlc + Ky	5.1355	Ky ($Si_1Al_2O_5$)
	0.0287	O
⇒	2.6251	Crd ($Si_{4.984}Al_{3.975}Ti_{0.000}Fe_{0.016}Mn_{0.001}Mg_{2.027}Ca_{0.004}Na_{0.024}K_{0.004}O_{18}$)
	0.3898	Spr ($Si_{0.756}Al_{4.484}Ti_{0.002}Fe_{0.166}Mn_{0.000}Mg_{1.584}Ca_{0.000}Na_{0.003}K_{0.001}O_{10}$)
Crd + Spr + H_2O	1.9934	Fluid (H_2O)
		R ($Si_{0.000}Al_{0.000}Ti_{0.005}Cr_{-0.011}Fe_{0.042}Mn_{0.001}Mg_{0.000}Ca_{0.017}Na_{-0.035}K_{-0.001}F_{0.008}Cl_{0.004}$)

Tlc + Ky ⇒ Crd + Cor (**R**$_4$),

	1	Ta ($Si_{7.915}Al_{0.301}Ti_{0.010}Fe_{0.072}Mn_{0.000}Mg_{5.599}Ca_{0.018}Na_{0.000}K_{0.016}F_{0.125}Cl_{0.006}H_{3.868}O_{24}$)
Tlc + Ky	6.6042	Ky ($Si_1Al_2O_5$)
	0.1961	O
⇒		
	2.8998	Crd ($Si_{5.007}Al_{3.979}Ti_{0.002}Fe_{0.033}Mn_{0.003}Mg_{2.929}Ca_{0.010}Na_{0.059}K_{0.000}O_{18}$)
Crd + Cor + H_2O	0.9848	Cor (Al_2O_3)
	1.9340	Fluid (H_2O)
		R ($Si_{0.000}Al_{0.000}Ti_{0.004}Cr_{0.000}Fe_{-0.024}Mn_{-0.001}Mg_{0.006}Ca_{-0.012}Na_{-0.176}K_{0.016}F_{0.125}Cl_{0.000}$)

It is important to note that the appearance of the reactions **R_3** and **R_4** is highly variable, since they are mostly controlled by element diffusion. The occurrence of both reactions in some microdomains (**Fig. 5**) seems to be the result of the same process which takes place progressively and led to the coexistence of different textures in a mosaic equilibrium [27, 28]. This is directly controlled by the alumina immobility during the reaction. A global process regrouping these reactions can be expressed as follows:

Ta + Ky $\Rightarrow$ Crd + Spr + Cor (**R_5**).

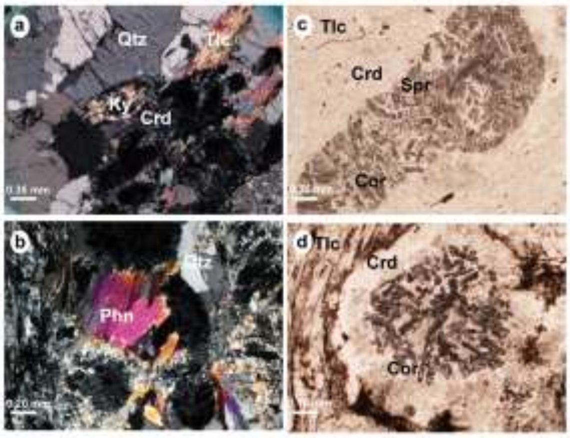

Fig 5. *Photomicrographs of typical minerals and textures of the studied whiteschists.*

a-b (Cross-polarized light): High-P talc + kyanite + quartz ± phengite paragenesis and its replacement by cordierite according to the limiting reaction Tlc + Ky + Qtz $\Leftrightarrow$ Crd.

c-d (plane-polarized light): Reaction microstructures after kyanite and talc showing the growth of cordierite + sapphirine ± corundum, or cordierite + corundum, during the high-T stage.

Consequently, corundum can grow together with sapphirine in the same symplectite and the products will create a coronitic texture surrounding the decreasing kyanite, composing of (**Figs. 5c** and **6**):

- A granulated polycrystalline aggregate of corundum-cordierite that dominates the inner part of the crown,
- A median aureole of sapphire-cordierite ± corundum,
- An outer aureole made of cordierite.

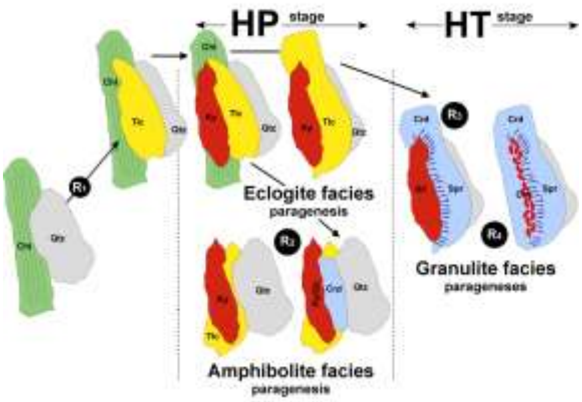

Fig 6. *Simplified diagram showing in summary the evolution of developed reactions and textures during the HP (high-pressure) and HT (high-temperature) stages, observed in the whiteschists of Ti-N-Eggoleh.*

The initial rock is assumed to be a chlorite (e.g. sudoite) and quartz-rich shale that reacted to generate talc and kyanite during a high-pressure prograde stage. As a result, the talc-kyanite-quartz paragenesis represents the peak of metamorphism in silica-rich rocks, while talc and kyanite are present in silica-deficient samples.

During the initial stages of decompression, cordierite replaces stable contacts between the early minerals following the R_1 in the silica-rich microdomains (amphibolites facies), whereas the contact between kyanite and talc remains stable in the quartz-free micromains.

The continued decrease of pressure together with a rise in temperature leads R_3 that gives sapphirine-cordierite symplectites from talc and kyanite and finally R_4, which led to the growth of corundum when kyanite is totally absorbed by the reaction.

III.2. Mineral chemistry

The chemical composition of the phases was determined using a Cameca SX100 electron microprobe at the University of Paris VI with operating conditions of 15 kV and 10 nA. Analyses were quantified using natural mineral standards and representative analyses of minerals are represented in Tables 1 and 2.

Tab 1. *Microprobe analyses of talc in quartz-bearing and quartz-free whiteschists*

Rock type	**Quartz-free whiteschists**								
Mineral	**Tlc**	**Tlc**	**Tlc**	**Tlc**	**Tlc**	**Tlc**	**Tlc**	**Tlc**	**Tlc**
SiO_2	55.61	55.98	56.07	56.70	57.49	57.72	58.12	58.33	58.62
Al_2O_3	2.71	1.86	2.31	1.88	1.12	2.05	1.65	1.88	1.52
Cr_2O_3	0.00	0.00	0.00	0.00	0.01	0.00	0.02	0.00	0.00
TiO_2	0.03	0.05	0.00	0.05	0.06	0.06	0.06	0.04	0.13
FeO	0.64	0.38	0.60	0.67	0.33	0.92	0.69	0.93	0.77
MgO	30.37	31.18	30.99	30.47	29.96	29.95	30.64	29.79	29.69
MnO	0.03	0.03	0.00	0.00	0.01	0.00	0.02	0.02	0.06
CaO	0.15	0.21	0.10	0.09	0.21	0.12	0.13	0.10	0.13
Na_2O	0.06	0.10	0.04	0.08	0.07	0.09	0.08	0.11	0.10
K_2O	0.04	0.04	0.01	0.03	0.00	0.02	0.03	0.03	0.03
P_2O_5	0.00	0.00	0.04	0.02	0.02	0.00	0.00	0.00	0.00
F	0.20	0.16	0.12	0.27	0.28	0.00	0.00	0.04	0.00
Cl	0.01	0.03	0.02	0.01	0.00	0.03	0.02	0.02	0.00
NiO	0.06	0.08	0.00	0.07	0.01	0.01	0.04	0.03	0.00
Sum	89.96	90.12	90.36	90.37	89.65	91.06	91.51	91.38	91.07

Rock type	**Quartz-bearing whiteschists**								
Mineral	**Tlc**	**Tlc**	**Tlc**	**Tlc**	**Tlc**	**Tlc**	**Tlc**	**Tlc**	**Tlc**
SiO_2	62.60	62.82	62.22	62.97	62.48	62.69	63.23	62.54	62.59
Al_2O_3	0.95	0.70	0.78	0.60	0.61	0.62	0.65	0.85	2.03
Cr_2O_3	0.00	0.00	0.05	0.03	0.00	0.04	0.00	0.00	0.06
TiO_2	0.02	0.00	0.04	0.00	0.11	0.04	0.08	0.03	0.10
FeO	0.16	0.48	1.54	0.75	0.13	0.16	0.78	0.83	1.16
MgO	30.71	30.22	29.87	31.19	30.99	31.19	29.81	30.90	29.44
MnO	0.00	0.00	0.00	0.00	0.06	0.02	0.12	0.00	0.11
CaO	0.03	0.00	0.02	0.06	0.03	0.03	0.10	0.03	0.12
Na_2O	0.23	0.18	0.14	0.16	0.15	0.22	0.16	0.08	0.08
K_2O	0.04	0.00	0.01	0.05	0.05	0.05	0.02	0.01	0.11
P_2O_5	0.00	0.00	0.04	0.07	0.03	0.08	0.01	0.01	0.00
F	1.17	1.03	0.00	0.52	0.67	1.25	0.22	0.00	0.37
Cl	0.02	0.01	0.00	0.00	0.02	0.03	0.02	0.00	0.01
NiO	0.00	0.00	0.00	0.00	0.00	0.00	0.02	0.00	0.00
Sum	96.01	95.44	94.78	96.45	95.34	96.45	95.39	95.37	96.21

Talc shows variable compositions. In General, the X_{Mg}-values $[Mg^{2+}/(Mg + Fe^{2+})]$ of talc vary from sample to sample (0.92 to 0.99). Talc from quartz-free whiteschists (**Tab. 1**) is more iron-rich (X_{Mg}: 0.92-0.96) than talc from quartz-bearing rocks (X_{Mg}: 0.95-0.99, **Fig.7 a**). This latter includes a higher content of silica in its structure (**Fig. 7b**). However, the Al-contents remain homogeneous in all samples (**Fig. 7c**).

Talc grains show slight alumina zoning (**Tab. 1**). Peak-stage talc contains 1% alumina, while the amount of Al_2O_3 rises up to 2% toward the rims.

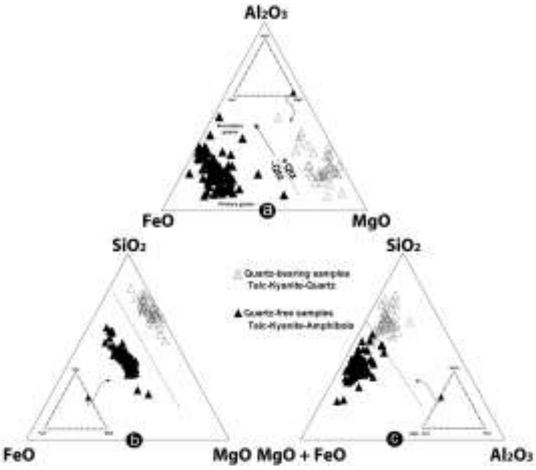

Fig 7. *Plotting talc composition in barycentric diagrams. (a): Alumina contents in talc are the same in both quartz-bearing and quartz-free samples (b): Talc is more Mg-rich in quartz-bearing than in quartz-free samples.* (c): Silica content in talc is significantly higher in quartz-bearing samples than in silica-poor rocks.

Amphibole: According Leake [29], amphibole is a magnesian tremolite (Si > 7.5, X_{Mg} > 0.95) containing a low alumina content (< 0.5).

The F and Cl amounts are also low (< 0.013 and < 0.121, respectively), and the TiO_2 amount is almost negligible too (< 0.045) [25].

Tab 2. *Microprobe analyses of phengite, sapphirine and cordierite*

Minéral	**Phn**	**Phn**	**Spr**	**Spr**	**Crd**	**Crd**
SiO_2	44.45	46.09	10.76	10.86	51.21	50.47
TiO_2	0.00	0.00	0.08	0.00	0.00	0.00
Al_2O_3	31.65	30.60	70.01	70.03	33.86	34.17
Cr_2O_3	0.01	0.07	-	-	-	-
FeO	1.02	0.64	0.29	0.41	0.66	0.61
MnO	0.02	0.02	0.03	0.01	0.00	0.02
MgO	7.25	4.18	18.60	18.56	13.01	13.22
CaO	0.06	0.05	0.02	0.01	0.06	0.08
Na_2O	0.13	0.09	0.03	0.01	0.15	0.18
Ka_2O	10.13	10.35	0.00	0.08	0.00	0.00
F	0.00	0.00	-	-	-	-
Cl	0.01	0.04	-	-	-	-
Sum	94.73	92.13	99.83	99.97	99.06	99.08

Mica corresponds to a Mg-rich phengite ($X_{Mg} \approx 0.92$), containing a low and constant silica content (5.8-6.2 cations, for 22 oxygens).

The alkali amounts are constant, mostly Na (0.023 < Na < 0.044 and 1.250 < K < 1.550).

In some samples, the composition of this mica is peculiar since it approximates both of phlogopite and phengite. This is most likely due to the evolution of phlogopite in to phengite. Such a transformation is specific to the high-pressure environments.

Cordierite is particularly magnesian, as it approaches the Mg^{Crd} end-member ($2MgO:2Al_2O_3:5SiO_2$). The X_{Mg} ratio is about 0.99 in all samples (**Tab. 2**).

Sapphirine: Only coarse sapphirine-symplectites have been analysed. Semiquantitative EDS analyses reveal that alumina contents in symplectites found in contact with sillimanite are significantly elevated, but could not be analysed by microprobe. Generally, the silica decreasing is accompanied by increasing of alumina from the coarsest to the finest symplectites, which surround silimanite or are directly in contact with corundum that replaces kyanite in the last stage of retromorphosis. A remarkable feature is that the highest alumina content in sapphirine is found in quartz-bearing samples, where remnants of alumino-silicate are preserved, and retromorphosis is rather less advanced compared to quartz-free samples (**Tab. 2**).

Therefore, microprobe analysis of this sapphirine allows to define it as one of most aluminous of the world, and places it beyond the 13(Mg, Fe)O : 19(Al, Cr, Fe^{3+}) : 5(SiO_2) end-member.

The Fe^{3+} content, as estimated by Higgins [30], is low ($Fe^{3+} < 0.04$) or absent and the chrome content is negligible (< 0.016).

For many authors, the presence of chrome is required to keep the stability of this type of sapphirine (considered as metastable), by substituting alumina.

Accessory minerals

Apatite is particularly fluorine rich (≈ 4%) and rutile may contain significant amounts of Cr_2O_3 (0.10-1.70 %). A minor amount of iron is found in kyanite (0.10%) and corundum (0.40%). This last may contain also some titanium (0.12%).

III.3. P-T Formation environment

It is generally difficult to analyze the prograde P-T history for strongly retrograded rocks, because the mineral formed during the prograde stage are commonly completely replaced by peak and retrograde assemblages.

Despite the pervasive strong retrogression, the Ti-N-Eggoleh whiteschists preserve information on the prograde metamorphic stage, as demonstrated by the presence of relicts of talc, kyanite, quartz and a few phengite in some rare samples.

Based on experimental data and the established phase relationships in the MAS(H) and FMAS(H) systems, the main observations concerning the studied rocks are the following (**Fig. 8**):

- The absence of carpholite is due to HT conditions recorded during the later stage of the metamorphic evolution, which obliterates low-grade parageneses, restricted by specific temperature boundaries.
- The absence of chloritoid would indicate that pressure may not have exceeded 25 kbar, along the metamorphic evolution, given that the chemistry of these rocks perfectly adequate for the development of this mineral.
- The absence of coesite supports this assumption and suggests a P < 25 kbar during the peak-stage eclogitic metamorphism.
- The absence of yoderite can be justified by the silica-environment which is not favorable to the occurrence of this mineral.
- The absence of staurolite must be related, in particular, to the highly Mg-rich composition of the rock. Indeed, Al_2O_3 deficiency may not be a barrier in this case, since kyanite, sapphirine and corundum, are common in this environment. It is possible that P is a determining factor too, since staurolite becomes metastable at P < 13 kbar.

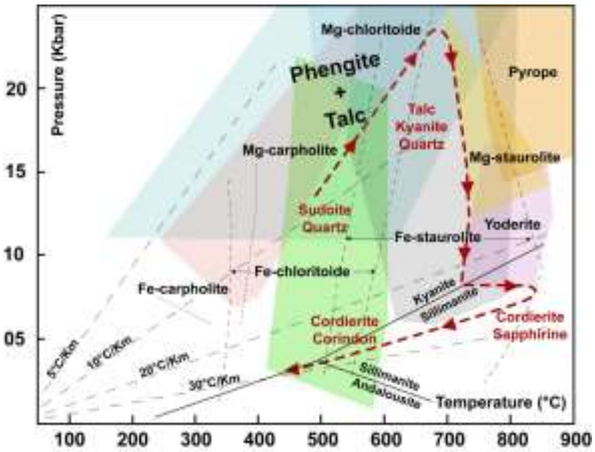

Fig 8. Pressure-temperature diagram for whiteschists.

The stability domains of various minerals that may occur in whiteschists are superposed to define a intermediate path that runs across fields corresponding to our textures.

These P-T ranges are based on the experimental works of [31, 32, 33, 34, 35, 36] that were carried in the (K)MASH system.

According to the P-T trajectory defined on the basis of the observable textures and reactions, a prograde stage allows the stability of the talc-kyanite-quartz paragenesis at P close to 20 Kbar. Above this pressure, Mg-chlorite and staurolite end-memebers become stabilized in the rock, which is not the case in the studied rocks. The development of late cordierite-sapphirine and cordierite-corundum symlectites requires decompression from 10 kbar. A rise in temperature is required in such cases [25].

As a result, it may be supposed that staurolite disappeared during late HT stage. It may also explain the absence pyrope, whose stability limit is situated at 15 kbar.

From the above, the following evolution pattern may be envisaged to recapitulate the metamorphic history of the Ti-N-Eggoleh whiteschists:

A prograde episode, characterized by an increasing P up to a maximum of 20-25 kbar, *i.e.* below the quartz-coesite transition. These conditions allow the growth and stability of talc-kyanite-quartz. This event is succeeded by a decrease of pressure up to 13 kbar, and then an increasing of T during exhumation.

IV. Conclusion

High-P environment terranes are recognized in several collisional zones in the African continent.

Whiteschists typically are found in Alpine-type orogens, e.g., Western Alps, Trans-Himalaya (Sar e Sang - Afghanistan).

The main paragenesis in the Ti-N-Eggoleh whiteschists (Central Hoggar, Algeria) consists of talc + kyanite ± quartz which has a wide P–T stability environment that ranges from high-P amphibolite to eclogite facies. Cordierite, sapphirine and corundum formed at the contact between kyanite and talc through metamorphic reactions produced complex symplectites and coronae. These newly formed minerals are typical of a high-T evolution. These reactions occurred at P–T conditions between 7 kbar–630 °C and 11 kbar–820°C, during the transition to granulite facies conditions (**Fig. 9**).

Thus, the Ti-N-Eggoleh talc schists preserve information concerning both the peak and retrograde stages of metamorphism. The combination of mineral zoning (the high degree of Tschermak substitution in sapphirine, and in talc, which shows a secondary enrichment in Al at the rims of primary flakes), textural features, and P-T estimates allows the reconstruction of a clockwise P-T path, which shows that these whiteschists were subducted to great depth (**Fig. 9**).

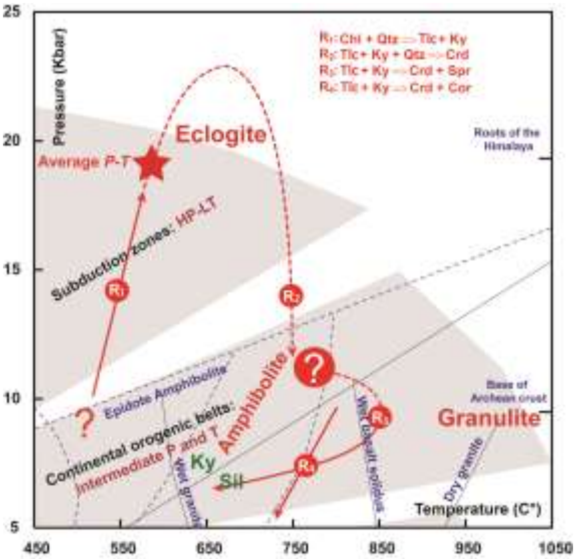

Fig 9. *P-T path of the Ti-N-Eggoleh whiteschists in relation with the geodynamic context. Reactions described above are projected in order to establish a relation between the corresponding tectonic episode and the type of transformation [25].*

These results are consistent, too, with the closure of an oceanic basin and ends with an orogeny that likely occurred during amalgamation of the various segments of the Tuareg Shield that happened during the Pan-African orogeny. When the collision came to an end, rapid erosion and/or tectonic uplift followed, leading to a delamination of the lithosphere and an upwelling of the asthenosphere. This induced a significant heat transfer and caused a granulitic metamorphism during the post-collisional stage (**Fig. 9**).

V. References

1. Sharp, Z. D.; Essene, E. J.; Hunziker, J. C. Stable isotope geochemistry and phase equilibria of coesite-bearing whiteschists, Dora Maira Massif, western Aps. *Contributions to Mineralogy and Petrology* 114 (1993) 1-12.
2. Schreyer, W.; Abraham, Kurt. Three-stage metamorphic history of a white schist from Sare Sang, Afghanistan, as part of a former evaporite deposit. *Contributions to Mineralogy and Petrology* 59 (1976) 111-130.
3. Hubbard, M. S.; Grew, E. S.; Hodges, K. V.; Yates, M. G.; Pertsev, N. N. Neogene cooling and exhumation of upper-amphibolite-facies 'whiteschists' in the Southwest Pamir Mountains, *Tajikistan. Tectonophysics* 305 (1999) 325-337.
4. Johnson, S. P.; Oliver, G. J. H. Mesoproterozoic oceanic subduction, island-arc formation and the initiation of back-arc spreading in the Kibaran Belt of central, southern Africa: evidence from the Ophiolite Terrane, Chewore Inliers, northern Zimbabwe. *Precambrian Research* 103 (2000) 125-146.
5. Parkinson, C. D.; Zhang, R.Y.; Liou, J.G. A unique record of progressive UHP metamorphism and whiteschists of the Kulet region. In: Parkinson, C.D., Katayama, I.; Liou, J. G.; Maruyama, S. (Eds.). The diamond-bearing Kokchetav Massif, Kazakhstan; petrochemistry and tectonic evolution of an unique ultrahigh-pressure metamorphic terrane. Frontiers Science Series, *Universal Academy*: Tokyo, Japan, (2000) 321-342.
6. Munz, I.A. Whiteschists and orthoamphibole-cordierite rocks and the *P-T-t* path of the Modum Complex, south Norway. *Lithos* 24 (2000) 181-199.
7. Rolfo, F.; Compagnoni, R.; Xu, S.; Jiang, L. First report of felsic whiteschists in the ultrahigh-pressure metamorphic belt of Dabie Shan, China. *European Journal of Mineralogy* 12 (2000) 883-898.
8. Pawlig, S.; Baumgartner, L. P. Geochemistry of a talc–kyanite–chloritoid shear zone within the Monte Rosa granite, Val d'Ayas, Italy.*Schweizerische ineralogische und Petrographische Mitteilungen* 81 (2001) 329-346.
9. Adjerid, Z.; Godard, G.; Ouzegane, K. High-pressure whiteschists from the Ti-N-Eggoleh area (Central Hoggar, Algeria): A record of Pan-African oceanic subduction. *Lithos* 31 (2015) 201-216.
10. Franz, L.; Romer, R. L.; De Capitani, C. Protoliths and phase petrology of whiteschists. *Contributions to Mineralogy and Petrology* 166 (2013) 255-274.
11. Liégeois, J.P. A new synthetic geological map of the Tuareg Shield: an overview of its global structure and geological evolution. In: Bendaoud, A., Hamimi, Z., Hamoudi, M., Djemai, S.; Zoheir, B. (Eds.). The

Geology of the Arab World - An Overview. Springer, *Verlag*, pp. (2019) 83-107.
12. Liégeois, J. P.; Abdelsalam, M. G.; Ennih, N.; Ouabadi, A. Metacraton: nature, genesis and behavior. *Gondwana Research* 23 (2013) 220-237.
13. Caby, R. Terrane assembly and geodynamic evolution of central-western Hoggar: a synthesis. Journal of African Earth Sciences, *Journal of African Earth Sciences* 37: (2003) 269-293.
14. Fezaa, N.; Liégeois, J. P.; Abdallah, N.; Cherfouh, E. H.; De Waele, B.; Bruguier, O.; Ouabadi, A. Late Ediacaran geological evolution (575–555 Ma) of the Djanet Terrane, Eastern Hoggar, Algeria; evidence for a Murzukian intracontinentalepisode. *Precambrian Research* 180 (2010) 299-327.
15. Liégeois, J. P.; Latouche, L.; Boughrara, M.; Navez, J.; Guiraud, M. The LATEA metacraton (Central Hoggar, Tuareg shield, Algeria): Behaviour of an old passive margin during the Pan-African orogeny. *Journal of African Earth Sciences* 37 (2003) 161-190.
16. Ouzegane, K.; Guiraud, M.; Kienast, J. R. Prograde and retrograde evolution in high-temperature corundum granulites (FMAS and KFMASHsystems) from in Ouzzal Terrane (NW Hoggar, Algeria). *Journal of Petrology* 44 (2003) 517-545.
17. Peucat, J. J.; Drareni, A.; Latouche, L.; Deloule, E.; Vidal, P. U–Pb zircon (TIMS and SIMS) and Sm–Nd whole-rock geochronology of the Gour Oumelalen granulitic basement, Hoggar massif, Tuareg Shield, Algeria. *Journal of African Earth Sciences* 37 (2003) 229-239
18. Black, R.; Latouche, L.; Liégeois, J.P.; Bertrand, J.M. Pan-Africain displaced terranes in the Tuareg shield (central Sahara). *Geology* 22 (1994) 641-644.
19. Dostal, J.; Caby, R.; Keppie, J.D.; Maza, M., Neoproterozoic magmatism in Southern Algeria in Southern Algeria (Sebkha el Mehla inlier): A northern extension of the Trans Saharian orogenese. *Journal of African Earth Sciences* 35 (2002) 213-225.
20. Bertrand, J. M. L.; Caby, R. Geodynamic evolution of the Pan-African orogenic belt; a new interpretation of the Hoggar Shield (Algerian Sahara). *Geologische Rundschau* 67 (1978) 357-388.
21. Abdallah, N.; Liégeois J. P.; De Waele B.; Fezaa, N.; Ouabadi, A. The Temaguessine Fe-cordierite orbicular granite (Central Hoggar, Algeria): U–Pb SHRIMP age, petrology, origin and geo-dynamical consequences for the late Pan-African magmatism of the Tuareg shield. *Journal of African Earth Sciences* 49 (2007) 153-178.
22. Bitam-Derridj, A.; Ouzegane, K.; Adjerid, Z.; Godard, G.; Kienast, J.R. Les éclogites granulitisées de Ti-N-Eggoleh (terrane du Sérouènout, Hoggar central) : étude métamorphique et conséquence géodynamique. *Bulletin du Service Géologique National [Algérien]* 21 (2010) 117-136.
23. Adjerid, Z.; Ouzegane, K.; Godard, G.; Bitam-Derridj, A.; Kiénast, J.R. Le Sérouènout: Un fragment de lithosphère océanique subducté à haute pression, exhumé, puis granulitisé à haute température. *Bulletin du Service Géologique National [Algérien]* 23 (2012) 199-217.
24. Guérangé, B. L'Antécambrien de Temasin, Rapport du Bureau de Recherches Géologiques et Minières, (1966) 56 p.
25. Adjerid, Z. Textures et modélisation thermodynamique : Exemple des séries métamorphiques de haute température et de haute pression du Hoggar. Thèse de doctorat. FSTGAT-USTHB. (2009) 480p
26. Schreyer, W.; Abraham, Kurt. Three-stage metamorphic history of a white schist from Sare Sang, Afghanistan, as part of a former evaporite deposit. *Contributions to Mineralogy and Petrology* 59 (1976) 111-130.
27. Thompson, J. B. Local equilibrium in metasomatic processes. In *Researches in Geochemistry* (ed. Abelson, P. H.), (1959) pp 427–457. Wiley, New York.
28. Korzhinskii, D. S. Physicochemical Basis of the Analysis of the Paragenesis of Minerals. *Consultants Bureau, New York*, (1959) 142 pp.
29. Leake, B.E.; Woolley, A.R.; Birch, W.D.; Gilbert, M.C.; Grice, J.D.; Hawthorne, F.C.; Kato, A.; Kisch, H.J.; Krivovichev, V.G.; Linthout, K.; Laird, J.; Mandarino, J.; Maresch, W.V.; Nickel, E.H.; Rock, N.M.S.; Schumacher, J.C.; Smith, D.C.N.; Ungaretti, L.; Whittaker, E.J.W.; Youzhi, G. Nomenclature of amphiboles. *Canadian Mineralogist* 9 (1997) 623-651
30. Higgins, J. B.; Ribbe, P. H. Sapphirine II: a neutron and X-ray diffraction study of $(Mg–Al)^{VI}$ and $(Si–Al)^{IV}$ ordering in monoclinic sapphirine. *Contributions to Mineralogy and Petrology* 68 (1979) 357-368.
31. Schreyer, W.; Seifert, K. Compatibility relations of the aluminum silicates in the systems $MgO-Al_2O_3-SiO_2-H_2O$ and $K_2O-MgO-Al_2O_3-SiO_2-H_2O$ at high pressures. *American Journal of Sciences* 267 (1969) 371-388.
32. Kitahara, S.; Takenouchi, S.; Kennedy, G.C. Phase relations in the system $MgO-SiO_2-H_2O$ at high temperatures and pressures, *American Journal of Sciences* 264 (1966) 223-233.
33. Chopin, C.; Schreyer W. Magnesiocarpholite and magnesiochloritoid: two index minerals of pelitic blueschists and their preliminary phase relations in the model system $MgO-A1_2O_3-SiO_2-H_2O$. *American Journal of Sciences* 283 (1983) 72-96
34. Halbach, H.; Chaterjee, N. D. The use of linear parametric programming for determining internally consistent thermodynamic data for minerals. In: *High-pressure Resarches in Geoscience (ed. Schreyer, W.*), (1982) pp 475-491. Schweizerbart, Stuttgart.
35. Chopin, C. Coesite and pure pyrope in high-grade blueschists of the western Alps: A first record and some consequences, *Contributions to Mineralogy and Petrology*. 86 (1984) 107-118.
36. Fransolet, A. M.; Schreyer, W. Sudoite di/trioctahedral chlorite: a stable low-temperature phase in the system $MgO-Al_2O_3-SiO_2-H_2O$. *Contributions to Mineralogy and Petrology*. 86 (1984) 409-417.

Please cite this Article as:
Bitam-Derridj A., Adjerid Z., Ouzegane K., Formation environment of whiteschists from the Ti-N-Eggoleh region (Serouenout terrane, Central Hoggar): Petrographic, Mineralogical study and Estimation of P-T conditions. ***Algerian J. Env. Sc. Technology*, 9:4 (2023) 3334-3343**